

# Analysing the Surface Features of Samples with an Atomic Force Microscope

Katie Archer

February 25, 2025

## Abstract

Here we inspect the surface features of a calibration grid and CD using the static mode of an atomic force microscope, and use the dynamic mode on a surface capacitor array. We measure a scratch on the grid surface as  $0.98 \pm 0.04\mu\text{m}$  wide and  $16.93 \pm 0.09\text{nm}$  deep, and observe two possible pieces of atmospheric dust that are 131nm and 172nm tall. We observe the track and pit structure of the CD, measuring the track separation to be  $1.53 \pm 0.02\mu\text{m}$ , and note the discrete distribution of pit lengths. The field effect transistors on the surface capacitor array were located and their dimensions measured, with length  $10.05\mu\text{m}$  and two channel depths found to be 169nm and 124.3nm. We propose further lines of investigation into the features of these samples.

## Contents

<b>1</b>	<b>Introduction</b>	<b>2</b>
<b>2</b>	<b>Theory</b>	<b>2</b>
<b>3</b>	<b>Experimental Details</b>	<b>3</b>
<b>4</b>	<b>Experimental Results and Discussion</b>	<b>4</b>
<b>5</b>	<b>Conclusions</b>	<b>10</b>

# 1 Introduction

The atomic force microscope (AFM) was introduced by Binnig et al. in 1986[1] as an alternative to the scanning tunneling microscope (STM), which was limited to use on samples that were electrically conductive. It is part of the larger family of instruments called “scanning probe microscopes”, and is also known as the scanning force microscope. Due to its versatility, the AFM has become ubiquitous in the field of surface science.[2]

The objective of this experiment is to utilise AFMs to observe the surface topology of a calibration grid, a CD, and a switched capacitor array over areas on the scale of  $10^{-10}m^2$ . It is also the intention to obtain dimension measurements, such as heights and widths, from these for the small scale structures observed, both those we expect but also any surface aberrations due to damage, corrosion, or contaminants.

# 2 Theory

The AFM uses an ultralight probe tip at the end of a cantilever arm to scan over a surface with up to sub-nanometer resolution by physically touching the sample at points in a 2D grid of pixels. As a result, it does not require the sample to be electrically conducting, or even to be opaque. Additionally it can operate in an atmospheric or fluid environment, whereas a STM requires a vacuum. The force required to move the probe by measurable distances, on the order of  $10^{-6}\text{\AA}$ , can be as small as  $10^{-18}\text{N}$ . This allows the AFM to be sensitive to forces as small as those between atoms.[1]

One common mode of operation, referred to as ‘static’, involves sliding the probe tip over the sample surface. As it encounters surface features, the tip is pushed up and down, as well as being twisted laterally. A laser shining on the tip is reflected in different directions depending on the perturbed tip orientation, and is detected by a 2x2 grid of photodiodes. Combining the intensity data across all 4 allows the height and deflection of the tip to be calculated, and used to plot heightmaps and deflection images. Typically these will use a colour transition between light and dark to indicate the magnitude of the quantity at each pixel.

However, this static method may not be suitable for particularly rough or delicate surfaces. In such cases, a ‘dynamic’ mode of operation is employed, where the probe tip is made to oscillate near to its resonant frequency. If the

AFM head is close enough, the end of this oscillating tip will make repeated contact with the surface, dampening its amplitude. When the laser detects a decrease in this amplitude, the microscope head can raise itself until the tip end no longer makes contact. With this method the AFM can scan a surface of inconsistent height without crashing the tip into raised regions, as well as the surface of a fragile sample without exerting enough force to damage it. [3]

### 3 Experimental Details

The AFM was first connected to its controller and switched on, then connected to its companion software. After that, the manual screws were used to raise the probe head up and provide sufficient clearance to slide the sample underneath on top of a grounded sample holder. Then the probe was manually lowered with the screws, using a bubble level to ensure all sides were lowered uniformly, until the probe tip shadow came into view on the camera feed. Next it was lowered carefully using the manual control over the servo motor, and then the final approach was completed automatically by the software. This was all done to ensure the delicate probe tip did not crash into the sample surface and become damaged. This was done with both a calibration grid and a CD disk sample using the AFM equipped with a static tip, and also for a switched capacitor array (SCA) using another with a dynamic tip. With the dynamic tip, the resonant frequency was first found by the software to calibrate itself.



Figure 1: The atomic force microscope on top of its dampening stand, with a CD fragment on sample holder directly underneath the microscope head.

The AFM setup was placed on top of a rubber dampening structure, all shown in Figure 1, in order to absorb vibrations which could affect our imaging results. All samples were first imaged at a 256x256 resolution over a square region of side length  $50\mu m$ , scanning at a rate of 1 second per line. After that, the rate and resolution were kept the same but the scanning area was decreased, to get zoomed in images on areas of interest.

## 4 Experimental Results and Discussion

The first sample investigated was the AFM calibration grid with  $10\mu m$  periodicity, shown next to a centimeter scale in Figure 2. The first region observed showed a clear grid pattern of squares with rounded corners, but also some significant irregular surface features, see the top half of Figure 3. The bottom half of the figure shows a different region without these aberrations.



Figure 2: The calibration grid sample used, with a centimeter scale for reference.

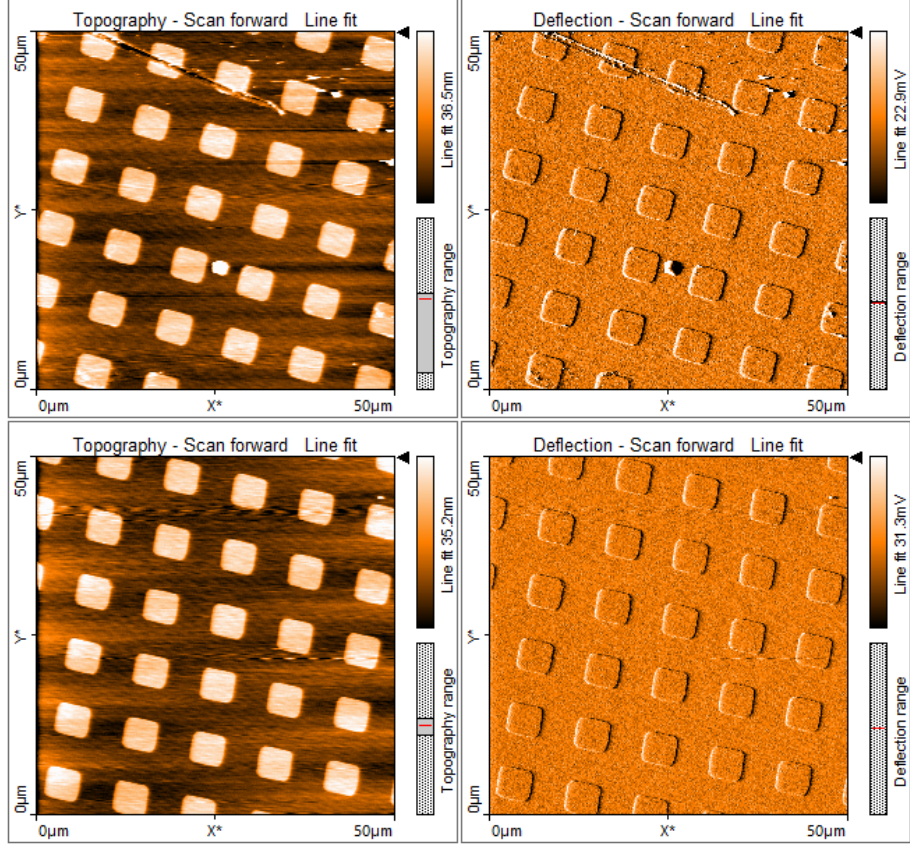


Figure 3: Results of the calibration grid scans, for the damaged (top) and clearer (bottom) sample regions, with the surface height (left) and deflection (right) shaded lighter for higher values.

The most notable of these unexpected features is a darker line appearing at the top of the image and stretching across several of the grid squares. Darker indicates deeper on this scale, so that would suggest that it is some kind of scratch or fissure in the surface of the sample. From the cross-section graph over a line perpendicular to the scratch in Figure 4, we can see that this scratch penetrates  $16.93 \pm 0.09\text{nm}$  below the average surface height of the raised squares. For reference, the thickness of a human hair is often taken to be around  $75\mu\text{m}$  [4], so the depth of this scratch is about 3 orders of magnitude smaller than that. The width of the scratch from the cross-section graph is  $0.98 \pm 0.04\mu\text{m}$ , but this is likely a slight overestimate as the line over which the cross-section was taken does not appear to be perfectly perpendicular to the direction of the scratch.

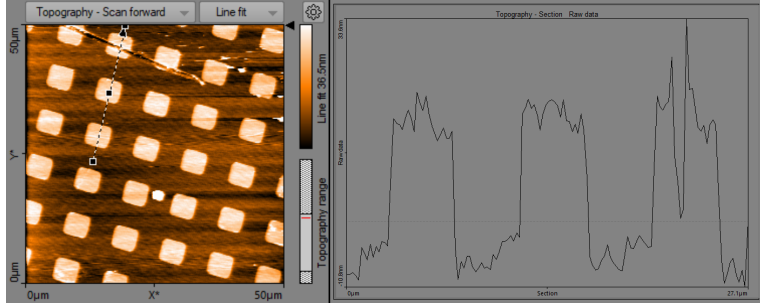


Figure 4: Height-map image (left) of the damaged region of the calibration grid, with a cross-section along the dashed line going across the scratch plotted (right).

The first scanned region also contained two roughly round and very bright features, their lightness indicating they extend relatively high above the rest of the surface. Cross sections through them both were taken, as shown in Figure 5, with the peak heights of the smaller and larger dots recorded at 131nm and 172nm respectively. Therefore these are comparatively very tall features. Based on their shape and size of  $\sim 0.1\mu\text{m}$ , they may be particles of atmospheric dust, however there are too many other possibilities to be certain.

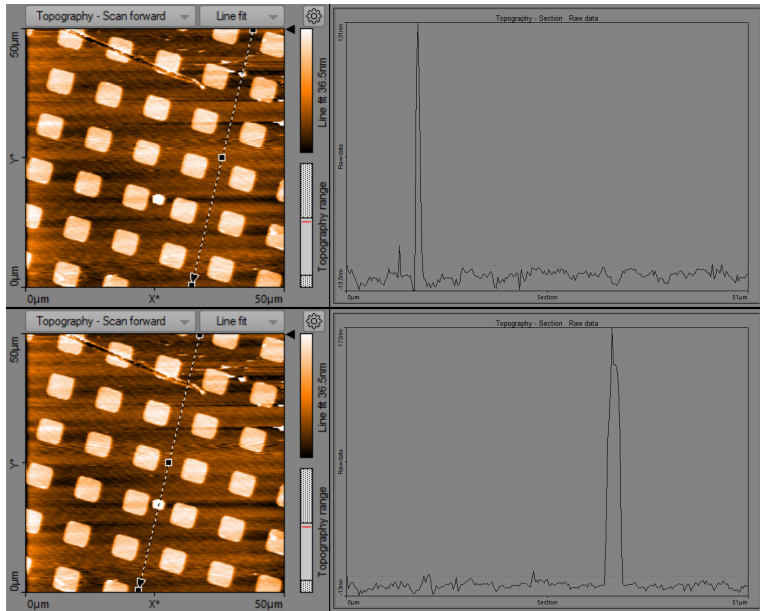


Figure 5: Cross-sections of the grid height-map through the small (top) and larger (bottom) particulates.

Zooming in on one of the scratched squares, shown in Figure 6, the width of one of the squares was measured to be  $4.806\mu\text{m}$ . Also, the periodicity of the grid squares was found to be  $9.71 \pm 0.01\mu\text{m}$ , close to the manufacturer claim of  $10\mu\text{m}$ .

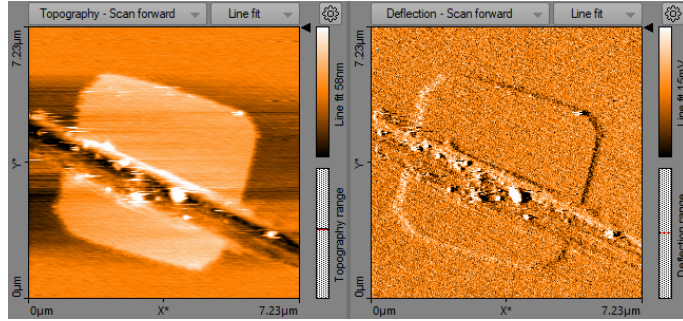


Figure 6: Close up scan of one of the scratched grid squares.

The second sample to be analysed was a fragment of a CD disk, which in a  $50 \times 50\mu\text{m}$  region appeared to contain about 40 tracks, each consisting of many pits of differing lengths. To closer inspect these features, we scanned a  $25 \times 25\mu\text{m}$  area, shown in Figure 7. The width between the tracks was found to be roughly constant across the scanned area, with the average separation between the centres of the tracks measured to be  $1.53 \pm 0.02\mu\text{m}$ . There seems to be a minimum length for the pits, and the longer pits appear to be 2, 3, or 4 times this length, without anything in between. It looks reasonable to assume that the pits and their separations are all integer multiples of this minimum length, as CDs are a digital storage medium and so would be expected to have the data on its surface quantized in regions of a size discernable by the sensitivity of the reading laser in a CD player.

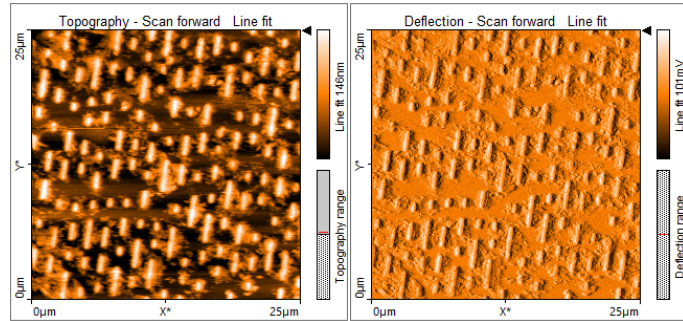


Figure 7: The AFM scan of the CD sample, with tracks and pits clearly visible.

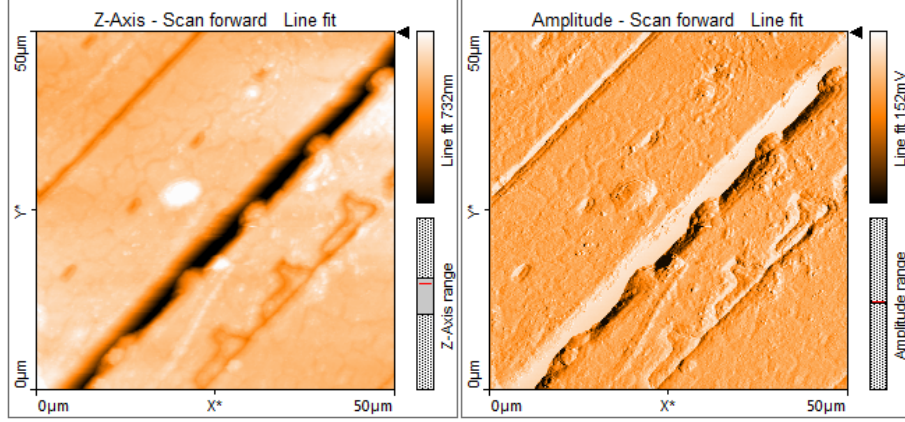


Figure 8: Dynamic AFM scan of the SCA sample, with the L-shaped FET structures visible in the bottom right quadrant of the scanned area.

The final sample was the SCA, and this was scanned using a dynamic tip, producing Figure 8. The L-shaped structures in the bottom right of the image are field effect transistors (FETs), and these are what we particularly wanted to investigate. Scanning over just one of these gave Figure 9, and from this we were able to measure the dimensions of the FET, finding it to be  $10.05\mu\text{m}$  long.

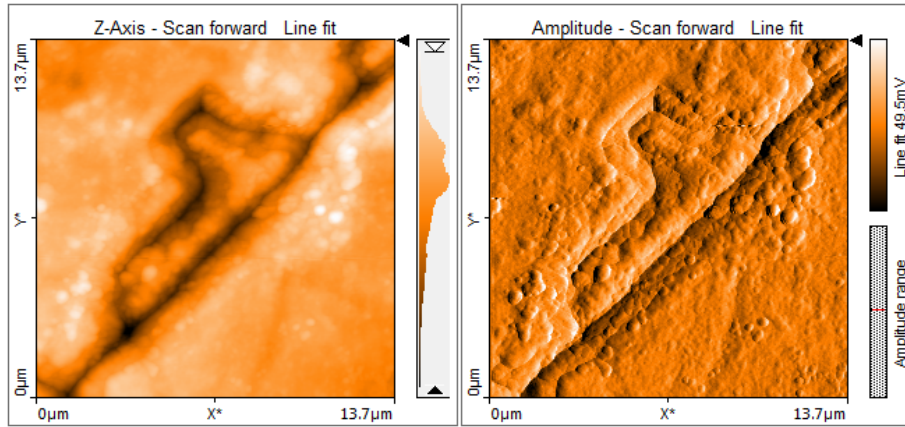


Figure 9: Close up scan of a single FET structure.

All of the measurements are shown on Figure 10. We also measured the cross-section across part of the FET in order to find the depths of the channels.

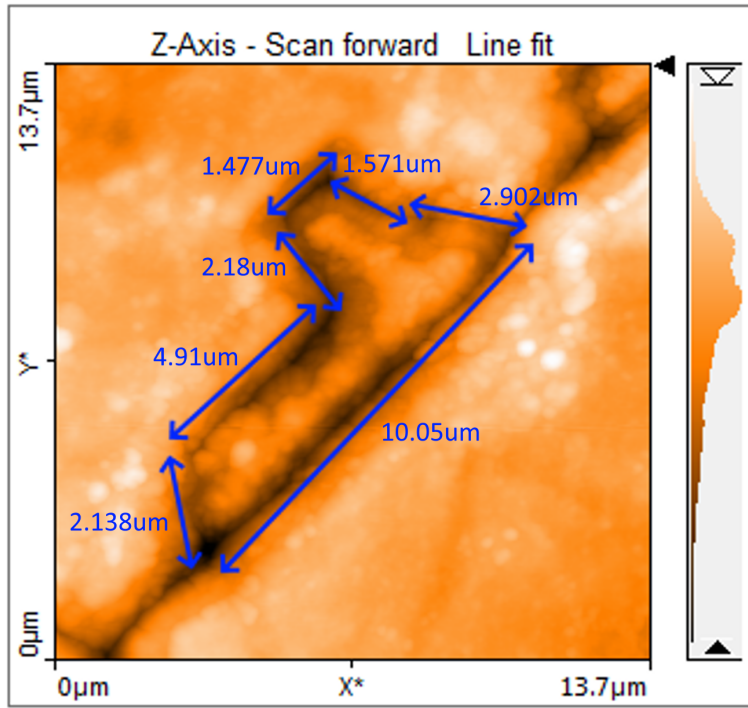


Figure 10: A scan of a FET structure with its measured dimensions overlaid on the image.

The cross-section line chosen crossed the edge of the FET twice (see Figure 11), giving us maximum depth values for the channel of 169nm and 124.3nm below the surface of the SCA.

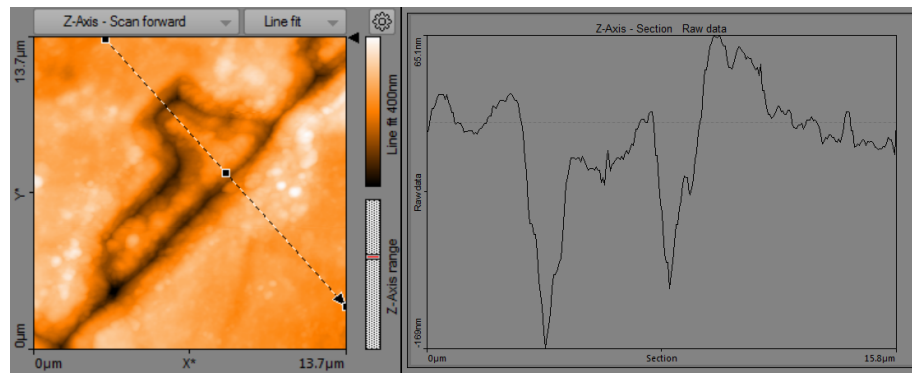


Figure 11: A cross-section taken along the dashed line shows the depths of the channels of the FET.

## 5 Conclusions

We were able to successfully image samples using the AFM. For the calibration grid, we were able to observe the repeating grid pattern, measure the width of a grid square as  $4.806\mu\text{m}$ , and determine the periodicity of the pattern to be  $9.71 \pm 0.01\mu\text{m}$ : a small disagreement from the supposed value. We investigated the size of 3 unexpected surface features, one which was deduced to be a very fine scratch  $0.98 \pm 0.04\mu\text{m}$  wide and  $16.93 \pm 0.09\text{nm}$  deep. The other two appear to be particulates of some nature, possibly atmospheric dust, with maximum heights above the surface of 131nm and 172nm. A further investigation these two features is made problematic by the imaging scale of the AFM, as it is unlikely the same small area could be found again. However, if these are indeed dust particulates, we expect there will be more across the surface of the sample, so these could be searched for. If the sample is held in place securely enough, it might be possible to raise the microscope head out of the way and clean the surface with compressed air without moving the sample. Then the same region could be scanned again to see if the ‘dust’ features persist, have moved, or disappeared entirely.

With the CD fragment, we measured a roughly constant distance between the centres of tracks of  $1.53 \pm 0.02\mu\text{m}$ , and observed that the pits seemed to all be integer multiples of some minimum pit length. As CDs are a digital medium, such discrete intervals are what we would expect. From their lightness in the images, the pits appear to be raised higher than the surrounding surface of the disk, suggesting that their name may be a historic misnomer. An area for further analysis could be making a comparison between CD samples from near the centre of the disk, and samples from the outer edge, to see whether the track separation remains constant, and to observe whether the minimum pit length changes. If the CD reader operates at a constant rotation rate, we would expect longer pits further out in order for the laser to read data at the same rate, but if it slows down for further out data the pits may be the same length as near the middle. We also might see this in the constant rotation case if the limiting factor is not the time resolution of the laser reader, but rather the physical scale limits of the manufacturing process.

An AFM was used in its ‘dynamic’ mode to scan an SCA, allowing us to observe the chain of L-shaped FET structures indented into the surface. Closer inspection allowed us to obtain dimensions for the FET’s channels, both in terms of horizontal lengths (see Figure 10), and vertical depths of 169nm

and 124.3nm. It would be interesting to see how these values vary, if at all, for the different FETs on the sample, and whether FETs on another sample have similar values or even the same shape.

## References

- [1] Binnig G, Quate C F, Gerber C. *Atomic force microscope*. Ridge, NY: American Physical Society; 1986.
- [2] Bowen W R, Hilal N. *Atomic force microscopy in process engineering introduction to AFM for improved processes and products*. Burlington, MA: Butterworth-Heinemann; 2009.
- [3] Haugstad G. *Atomic force microscopy exploring basic modes and advanced applications*. Hoboken, NJ: John Wiley & Sons; 2012.
- [4] Smith G T. *Industrial Metrology*. London: Springer London; 2002.